

## Electron-phonon interaction in anisotropic uniaxial double heterostructures

This article has been downloaded from IOPscience. Please scroll down to see the full text article.

1998 J. Phys.: Condens. Matter 10 3845

(<http://iopscience.iop.org/0953-8984/10/17/015>)

View [the table of contents for this issue](#), or go to the [journal homepage](#) for more

Download details:

IP Address: 171.66.16.209

The article was downloaded on 14/05/2010 at 13:03

Please note that [terms and conditions apply](#).

# Electron–phonon interaction in anisotropic uniaxial double heterostructures

E R Racec and D E N Brancus

Faculty of Physics, University of Bucharest, Bucharest, Romania

Received 1 December 1997, in final form 24 February 1998

**Abstract.** For a double semiconductor heterostructure having as interjacent layer an anisotropic uniaxial polar material with the optical axis directed along the normal to the interface, the eigenfrequencies and the eigenvectors of the field of the optical phonons are obtained in the context of the dielectric continuum model.

The form of the operator describing the interaction between the phonon modes and an electron is derived. The results are particularized to the case of a heterostructure made of zincblende-type semiconductors InP and GaAs with the pseudo-morphic layer uniaxially distorted by the built-in strain distribution.

## 1. Introduction

For a 3D system, many experimental and theoretical works have been done in the past to study the morphic effects (in particular those effects induced by a homogeneous stress distribution) in both the lattice dynamics and the electronic bands, respectively.

In the early 1980s the domain of the electronic properties of the strained-layer superlattices and afterwards that of the strained heterostructures came to the attention of the researchers due to their potentiality in manufacturing devices with enhanced performances. The high-speed modulation-doped field effect transistor (MODFET) and the low-threshold quantum well laser are two examples which benefited from the technique used to exploit the effects of the built-in strain distribution on the electronic properties of the semiconductor devices.

Apart from the case of the studies devoted to the electronic energy bands in strained heterostructures where both effects, that of the strain distribution and that of the confinement, are properly taken into account (Los *et al* 1996), the studies of the optical phonon modes and their interaction with the conduction electron in strained heterostructures present either the effect of the confinement according to theory developed by Mori and Ando (1989) for heterostructures made of isotropic materials or the effect of the strains, using the results obtained for 3D systems.

Investigating in the backscattering geometry the Raman spectra of the strained layers of GaAs which have estimated thicknesses of 18 and 28 Å and are grown on (001)-oriented InP substrates, Pistol *et al* (1992) have obtained a strain shift of the  $LO^{\Gamma}$  phonon frequency which agrees within 10% with the theoretical value predicted by continuum models (dielectric, elastic).

We present here, in the context of the dielectric continuum model, the phonon modes and their interaction with the conduction electron in an anisotropic semiconductor double

heterostructure (DHS). Based on the work of Pistol *et al* (1992) we apply our results to the cases of strained semiconductor heterostructures InP/GaAs/InP and GaAs/InP/GaAs obtained by growing the pseudo-morphic layers of GaAs and InP, uniaxially distorted, on the faces (001) and (111) respectively. We are limiting ourselves to the dielectric continuum model because the presence of the anisotropy and of the interfaces makes hopeless any attempt to improve the treatment along the lines of more elaborate models (Ridley *et al* 1994, Trallero-Giner *et al* 1992) considered for simpler systems.

## 2. Equations of the model

We consider a double heterostructure (DHS) of two polar crystals, labelled 1 and 2, for the sake of simplicity assumed diatomic, with the thicknesses  $l$  and  $l_2$ , verifying the inequality  $l \ll l_2$ .

According to figure 1 the material 1, lying between  $x_3 = \pm l/2$  with interfaces normal to the  $x_3$ -axis, is an anisotropic uniaxial crystal with the optical axis along  $x_3$ , and the material 2 is an isotropic one.

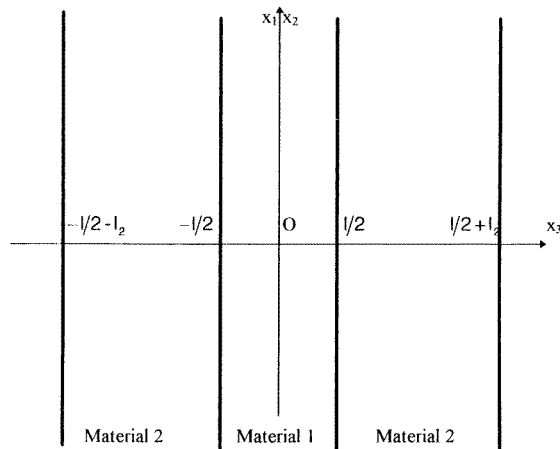


Figure 1. Geometry of the double heterostructure.

In the absence of free charges, the only two contributions to the total charge density are the bulk and the surface polarization charges. Thus, in the electrostatic approximation, the equation for the scalar potential is (Wendler 1985, Englman and Ruppin 1968):

$$\Phi(\mathbf{x}, t) = -\frac{1}{4\pi\epsilon_0} \sum_j \int d\mathbf{x}' \frac{\partial}{\partial x_j} \frac{1}{|\mathbf{x} - \mathbf{x}'|} P_j(\mathbf{x}', t) \quad (1)$$

where  $P(\mathbf{x}, t)$  is the electric polarization field.

To avoid the difficulty of obtaining an equivalent of the Lorentz relation between the local field and the macroscopic electric field, in this anisotropic case we are referring directly to the equations of the Born–Huang model: denoting the optical phonon field and the electric field by the vectors  $\mathbf{u}(\mathbf{x}, t)$  and  $\mathbf{E}(\mathbf{x}, t)$  respectively, the equations of the model are (Merten 1972):

$$\ddot{u}_i(\mathbf{x}, t) = \beta_{11,i}(x_3)u_i(\mathbf{x}, t) + \beta_{12,i}(x_3)E_i(\mathbf{x}, t) \quad (2a)$$

$$P_i(\mathbf{x}, t) = \beta_{12,i}(x_3)u_i(\mathbf{x}, t) + \beta_{22,i}(x_3)E_i(\mathbf{x}, t) \quad (2b)$$

$i = 1, 2, 3$ . In the system of equations (2), the coefficients  $\beta$ , in fact the elements of some diagonal matrices, (Merten 1972), are defined according to each domain of the heterostructure: isotropic/anisotropic/isotropic.

To allow a compact form of writing system (2) we introduce an  $x_3$ -dependence of the material parameters  $\beta$  by using the Heaviside function. Thus:

$$\beta_{11,i}(x_3) = -\omega_{TO,i}^2(x_3) \quad (3a)$$

$$\beta_{12,i}(x_3) = [\varepsilon_0(\varepsilon_i(0, x_3) - \varepsilon_i(\infty, x_3))]^{1/2} \omega_{TO,i}(x_3) \quad (3b)$$

$$\beta_{22,i}(x_3) = \varepsilon_0[\varepsilon_i(\infty, x_3) - 1] \quad (3c)$$

where, similar to the expressions of the dielectric constants along the principal directions  $\varepsilon_i(0, x_3)$  and  $\varepsilon_i(\infty, x_3)$ , for low and high frequency, respectively, the transverse-phonon mode frequencies  $\omega_{TO,i}(x_3)$  have the forms:

$$\omega_{TO,i}(x_3) = \omega_{TO}^{(2)}[H(-l/2 - x_3) + H(x_3 - l/2)] + \omega_{TO,i}^{(1)}[H(x_3 + l/2) - H(x_3 - l/2)] \quad (4)$$

and

$$H(x_3) = \begin{cases} 1 & x_3 \geq 0 \\ 0 & x_3 < 0. \end{cases} \quad (5)$$

The superscript indices (1) and (2) in the above expressions are referring to the anisotropic and isotropic domains of the heterostructure, respectively.

The equations (2) determine the components of the dielectric tensor:

$$\varepsilon_\alpha(\omega, x_3) = \varepsilon_\alpha(\infty, x_3) \frac{\omega_{LO,\alpha}^2(x_3) - \omega^2}{\omega_{TO,\alpha}^2(x_3) - \omega^2} \quad (6)$$

where  $\omega_{LO,\alpha}(x_3)$  are the longitudinal phonon mode frequencies along the principal directions; the index  $\alpha$  has been introduced to take into account the axial symmetry of the system, with  $\alpha = \perp$  for  $i = 1, 2$  and  $\alpha = \parallel$  for  $i = 3$ , the symbols  $\parallel$  and  $\perp$  corresponding to a direction that is either parallel or orthogonal to the optical axis, respectively. Following Wendler (1985) we introduce the Cartesian basis:

$$\begin{aligned} e_\perp(\mathbf{k}) &= \frac{k_1}{k} e_1 + \frac{k_2}{k} e_2 = \frac{\mathbf{k}}{k} \\ e_s(\mathbf{k}) &= \frac{k_2}{k} e_1 - \frac{k_1}{k} e_2 \\ e_\parallel &= e_3 \end{aligned} \quad (7)$$

which allows us to separate the field of phonons into an s-polarized part  $\mathbf{u}_s$  and a p-polarized part  $\mathbf{u}_p$ ,  $\mathbf{k}$  being the in-plane wave vector. Performing the two-dimensional Fourier transform used by Licari and Evrard (1977), for the components  $u_\perp$  and  $u_\parallel$  of  $\mathbf{u}_p$  one obtains the following system of integral equations:

$$\begin{aligned} g_\perp(\omega, x_3) u_\perp(\mathbf{k}, x_3, \omega) &= -\frac{k}{2} \int_{-l/2-l_2}^{l/2+l_2} dx'_3 e^{-k|x_3-x'_3|} [\chi_\perp(\omega, x'_3) g_\perp(\omega, x'_3) u_\perp(\mathbf{k}, x'_3, \omega) \\ &\quad + i \operatorname{sgn}(x_3 - x'_3) \chi_\parallel(\omega, x'_3) g_\parallel(\omega, x'_3) u_\parallel(\mathbf{k}, x'_3, \omega)] \end{aligned} \quad (8a)$$

$$\begin{aligned} \varepsilon_\parallel(\omega, x_3) g_\parallel(\omega, x_3) u_\parallel(\mathbf{k}, x_3, \omega) \\ = -\frac{k}{2} \int_{-l/2-l_2}^{l/2+l_2} dx'_3 e^{-k|x_3-x'_3|} [-\chi_\parallel(\omega, x'_3) g_\parallel(\omega, x'_3) u_\parallel(\mathbf{k}, x'_3, \omega) \\ + i \operatorname{sgn}(x_3 - x'_3) \chi_\perp(\omega, x'_3) g_\perp(\omega, x'_3) u_\perp(\mathbf{k}, x'_3, \omega)] \end{aligned} \quad (8b)$$

where

$$g_{\alpha}(\omega, x_3) = \frac{\omega_{TO,\alpha}^2(x_3) - \omega^2}{\beta_{12,\alpha}(x_3)} \quad (9)$$

$$\chi_{\alpha}(\omega, x_3) = \varepsilon_{\alpha}(\omega, x_3) - 1 \quad (10)$$

and

$$\text{sgn}(x_3 - x'_3) = \begin{cases} 1 & x_3 > x'_3 \\ -1 & x_3 < x'_3. \end{cases} \quad (11)$$

We are not taking into consideration the problem of the s-polarized part of the field of phonons which verifies the equation

$$g_{\perp}(\omega, x_3)u_s(\mathbf{k}, x_3, \omega) = 0 \quad (12)$$

because it does not interact with the conduction electron.

### 3. Normal modes

Following the procedure used by Wendler and Jäger (1983) which transforms the system (8) of Fredholm-type integral equations into differential equations, the eigenvectors and the eigenfrequencies of the field of phonons are obtained. Being solutions of the system of integral equations (8), the eigenvectors of the field of phonons satisfy the boundary conditions determined by the electrostatic theory (Englman and Ruppin 1968). Thus, at every interface of a heterostructure, the normal component of the displacement field and the tangential components of the electric field are conserved.

The equation for  $u_{\perp}$  is obtained by differentiating (8a) twice and replacing  $du_{\parallel}/dx_3$  by the derivative of (8b). It is easy to see that, strictly in this anisotropic uniaxial case,  $\omega_{LO,\perp}^{(1)}$ ,  $\omega_{LO,\parallel}^{(1)}$ ,  $\omega_{TO,\perp}^{(1)}$  and  $\omega_{TO,\parallel}^{(1)}$  are not eigenfrequencies of the field of phonons so that the obtained differential equations can be put in the form:

$$\frac{d^2}{dx_3^2}u_{\perp}(\mathbf{k}, x_3, \omega) = k^2 \frac{\varepsilon_{\perp}(\omega, x_3)}{\varepsilon_{\parallel}(\omega, x_3)}u_{\perp}(\mathbf{k}, x_3, \omega) \quad (13a)$$

$$u_{\parallel}(\mathbf{k}, x_3, \omega) = -\frac{i}{k} \frac{g_{\perp}(\omega, x_3)}{g_{\parallel}(\omega, x_3)} \frac{d}{dx_3}u_{\perp}(\mathbf{k}, x_3, \omega). \quad (13b)$$

Based on the equation (13a) one observes that depending on the sign of the ratio  $r(\omega) = \varepsilon_{\perp}^{(1)}(\omega)/\varepsilon_{\parallel}^{(1)}(\omega)$  and similar to the case of isotropic heterostructures (Mori and Ando 1989) the phonon modes are classified as interface modes for  $r(\omega) > 0$  and confined modes for  $r(\omega) < 0$ . Having the same solution as for isotropic heterostructures, the problem of so-called half-space modes (Mori and Ando 1989) was overlooked here.

Introducing into the integral equations (8) the solutions of the equations (13) (which forms depends on the particular domain of the heterostructures) both the dispersion laws and the form of the eigenmodes of the field of phonons are obtained.

#### 3.1. Interface modes

With the accomplishment of the supplementary condition

$$\varepsilon_{\parallel}^{(1)}(\omega)\varepsilon^{(2)}(\omega) < 0 \quad (14)$$

the frequencies  $\omega_{0,\mu,p}$  of the interface modes are the solutions of the equation:

$$\cosh[\gamma(\omega)kl] = p \frac{\varepsilon_{\perp}^{(1)}(\omega)\varepsilon_{\parallel}^{(1)}(\omega) + (\varepsilon^{(2)}(\omega))^2}{\varepsilon_{\perp}^{(1)}(\omega)\varepsilon_{\parallel}^{(1)}(\omega) - (\varepsilon^{(2)}(\omega))^2} \quad (15)$$

verifying, for the two values of the parity index,  $p$ , the conditions:

$$\varepsilon_{\perp}^{(1)}(\omega)\varepsilon_{\parallel}^{(1)}(\omega) > (\varepsilon^{(2)}(\omega))^2 \quad \text{for } p = + \quad (16a)$$

$$0 < \varepsilon_{\perp}^{(1)}(\omega)\varepsilon_{\parallel}^{(1)}(\omega) < (\varepsilon^{(2)}(\omega))^2 \quad \text{for } p = - \quad (16b)$$

where  $\gamma(\omega) = (r(\omega))^{1/2}$ .

The condition (14) introduces a branch index  $\mu$  taking the values 1 and 2 according to the sign of  $\varepsilon_{\parallel}^{(1)}(\omega)$ , positive and negative, respectively. The expressions of the interface mode eigenvectors,  $\mathbf{u}^{0,\mu,p}$ , are presented in table 1. As we shall see in section 5, for the particular case of a heterostructure made of materials having the *reststrahlen* bands well separated, the interface modes can be considered as interface-like substrate and interface-like pseudo-morphic layer modes.

**Table 1.** The eigenmodes for DHS considered.

Eigenvalues	Eigenvectors
$\omega_{m,\mu,+}$	$\mathbf{u}^{m,\mu,+}(\mathbf{k}, x_3) = C_{m,\mu,+} \left( -ik \frac{F_+(k, \omega_{m,\mu,+}, l, x_3)}{g_{\perp}(\omega_{m,\mu,+}, x_3)}, \right.$ $\left. k\gamma(\omega_{m,\mu,+}) \frac{\varepsilon_{\parallel}^{(1)}(\omega_{m,\mu,+})}{\varepsilon_{\parallel}(\omega_{m,\mu,+}, x_3)} \frac{F_-(k, \omega_{m,\mu,+}, l, x_3)}{g_{\parallel}(\omega_{m,\mu,+}, x_3)} \right)$
$\omega_{m,\mu,-}$	$\mathbf{u}^{m,\mu,-}(\mathbf{k}, x_3) = C_{m,\mu,-} \left( -ik \frac{F_-(k, \omega_{m,\mu,-}, l, x_3)}{g_{\perp}(\omega_{m,\mu,-}, x_3)}, \right.$ $\left. -k\gamma(\omega_{m,\mu,-}) \frac{\varepsilon_{\parallel}^{(1)}(\omega_{m,\mu,-})}{\varepsilon_{\parallel}(\omega_{m,\mu,-}, x_3)} \frac{F_+(k, \omega_{m,\mu,-}, l, x_3)}{g_{\parallel}(\omega_{m,\mu,-}, x_3)} \right)$
$\omega_{0,\mu,+}$	$\mathbf{u}^{0,\mu,+}(\mathbf{k}, x_3) = C_{0,\mu,+} \left( -ik \frac{F_{0,+}(k, \omega_{0,\mu,+}, l, x_3)}{g_{\perp}(\omega_{0,\mu,+}, x_3)}, \right.$ $\left. -k\gamma(\omega_{0,\mu,+}) \frac{\varepsilon_{\parallel}^{(1)}(\omega_{0,\mu,+})}{\varepsilon_{\parallel}(\omega_{0,\mu,+}, x_3)} \frac{F_{0,-}(k, \omega_{0,\mu,+}, l, x_3)}{g_{\parallel}(\omega_{0,\mu,+}, x_3)} \right)$
$\omega_{0,\mu,-}$	$\mathbf{u}^{0,\mu,-}(\mathbf{k}, x_3) = C_{0,\mu,-} \left( -ik \frac{F_{0,-}(k, \omega_{0,\mu,-}, l, x_3)}{g_{\perp}(\omega_{0,\mu,-}, x_3)}, \right.$ $\left. -k\gamma(\omega_{0,\mu,-}) \frac{\varepsilon_{\parallel}^{(1)}(\omega_{0,\mu,-})}{\varepsilon_{\parallel}(\omega_{0,\mu,-}, x_3)} \frac{F_{0,+}(k, \omega_{0,\mu,-}, l, x_3)}{g_{\parallel}(\omega_{0,\mu,-}, x_3)} \right)$

### 3.2. Confined modes in anisotropic layer

For the case  $r(\omega) < 0$  which determines the existence of periodical solutions (confined modes) in the anisotropic domain of the heterostructures the eigenfrequencies  $\omega_{m,\mu,p}$  are obtained as solutions of the equation:

$$\cos[\gamma(\omega)kl] = p \frac{\varepsilon_{\perp}^{(1)}(\omega)\varepsilon_{\parallel}^{(1)}(\omega) + (\varepsilon^{(2)}(\omega))^2}{\varepsilon_{\perp}^{(1)}(\omega)\varepsilon_{\parallel}^{(1)}(\omega) - (\varepsilon^{(2)}(\omega))^2} \quad (17)$$

satisfying the condition

$$kl\gamma(\omega_{m,\mu,p}) \in ((m-1)\pi, m\pi) \quad (18)$$

with  $\gamma(\omega) = |r(\omega)|^{1/2}$ . The parity and the branch indices are chosen according to the following rules:

$$\text{for } p = + \begin{cases} m = 1, 3, 5, \dots; \mu = 1 & \text{if } \varepsilon_{\parallel}^{(1)}(\omega)\varepsilon^{(2)}(\omega) > 0 \\ m = 2, 4, 6, \dots; \mu = 2 & \text{if } \varepsilon_{\parallel}^{(1)}(\omega)\varepsilon^{(2)}(\omega) < 0 \end{cases} \quad (19a)$$

$$\text{for } p = - \begin{cases} m = 2, 4, 6, \dots; \mu = 1 & \text{if } \varepsilon_{\parallel}^{(1)}(\omega)\varepsilon^{(2)}(\omega) > 0 \\ m = 1, 3, 5, \dots; \mu = 2 & \text{if } \varepsilon_{\parallel}^{(1)}(\omega)\varepsilon^{(2)}(\omega) < 0. \end{cases} \quad (19b)$$

The corresponding eigenvectors given in table 1 are periodical functions inside the anisotropic layer and strongly decrease with the distance to the interface outside the layer. For the different regions of the DHS the functions  $F_J$  have the expressions given in table 2.

**Table 2.** The functions  $F_J$  for the different regions of DHS.

$J$	$F_J$		
	$x_3 < -l/2$	$ x_3  \leq l/2$	$x_3 > l/2$
$J = +$	$\cos[k\gamma(\omega)l/2]e^{k(x_3+l/2)}$	$\cos[k\gamma(\omega)x_3]$	$\cos[k\gamma(\omega)l/2]e^{-k(x_3-l/2)}$
$J = -$	$-\sin[k\gamma(\omega)l/2]e^{k(x_3+l/2)}$	$\sin[k\gamma(\omega)x_3]$	$\sin[k\gamma(\omega)l/2]e^{-k(x_3-l/2)}$
$J = 0, +$	$\cosh[\gamma(\omega)kl/2]e^{k(x_3+l/2)}$	$\cosh[\gamma(\omega)kx_3]$	$\cosh[\gamma(\omega)kl/2]e^{-k(x_3-l/2)}$
$J = 0, -$	$-\sinh[\gamma(\omega)kl/2]e^{k(x_3+l/2)}$	$\sinh[\gamma(\omega)kx_3]$	$\sinh[\gamma(\omega)kl/2]e^{-k(x_3-l/2)}$

In contradistinction with the situation encountered for isotropic heterostructures when the confined modes are degenerate having the frequencies  $\omega_{TO}^{(1)}$  and  $\omega_{LO}^{(1)}$  (Mori and Ando 1989), for the anisotropic heterostructures discussed here, the degeneracy is lifted and the frequencies of the confined modes are distributed in two domains of frequency corresponding to the values  $\mu = 1, 2$  in the relations (19).

In the particular case of materials having *reststrahlen* bands well separated and in the limit of thick anisotropic layer, these domains are those of quasi-transverse modes ( $\omega$  between  $\omega_{TO,\parallel}^{(1)}$  and  $\omega_{TO,\perp}^{(1)}$ ) and quasi-longitudinal ones ( $\omega$  between  $\omega_{LO,\parallel}^{(1)}$  and  $\omega_{LO,\perp}^{(1)}$ ).

The normalized constants  $C_{m,\mu,p}$  and  $C_{0,\mu,p}$  used in table 1 have the expressions:

$$C_{m,\mu,p} = \left\{ \frac{\varepsilon_0 k^2}{4\omega} \left[ \frac{d\varepsilon_{\perp}^{(1)}}{d\omega} + \gamma^2(\omega) \frac{d\varepsilon_{\parallel}^{(1)}}{d\omega} + p \frac{\sin[\gamma(\omega)kl]}{\gamma(\omega)kl} \left( \frac{d\varepsilon_{\perp}^{(1)}}{d\omega} - \gamma^2(\omega) \frac{d\varepsilon_{\parallel}^{(1)}}{d\omega} \right) \right. \right. \\ \left. \left. + 2p \frac{\sin[\gamma(\omega)kl]}{kl} \frac{\gamma(\omega)\varepsilon_{\parallel}^{(1)}(\omega)}{\varepsilon^{(2)}\omega} \frac{d\varepsilon^{(2)}}{d\omega} \right] \Big|_{\omega=\omega_{m,\mu,p}} \right\}^{-1/2} \quad (20)$$

$$C_{0,\mu,p} = \left\{ \frac{\varepsilon_0 k^2}{4\omega} \left[ p \left( \frac{d\varepsilon_{\perp}^{(1)}}{d\omega} - \gamma^2(\omega) \frac{d\varepsilon_{\parallel}^{(1)}}{d\omega} \right) + \frac{\sinh[\gamma(\omega)kl]}{\gamma(\omega)kl} \left( \frac{d\varepsilon_{\perp}^{(1)}}{d\omega} + \gamma^2(\omega) \frac{d\varepsilon_{\parallel}^{(1)}}{d\omega} \right) \right. \right. \\ \left. \left. - 2 \frac{\sinh[\gamma(\omega)kl]}{kl} \frac{\gamma(\omega)\varepsilon_{\parallel}^{(1)}(\omega)}{\varepsilon^{(2)}\omega} \frac{d\varepsilon^{(2)}}{d\omega} \right] \Big|_{\omega=\omega_{0,\mu,p}} \right\}^{-1/2}. \quad (21)$$

The obtained eigenvectors verify a relation of orthonormality. All the eigenvectors of the DHS, the half-space modes included, satisfy a closure relation.

Developing the fields entering into the expression of the energy density (Brancus and Mocuta 1995), appropriate also for an anisotropic DHS, in terms of obtained eigenvectors, one finds the diagonal form of the Hamiltonian of optical phonons:

$$H_{ph} = \sum_{\mathbf{k}, m, \mu, p} \hbar \omega_{m,\mu,p}(\mathbf{k}) (a_{m,\mu,p}^+(\mathbf{k}) a_{m,\mu,p}(\mathbf{k}) + \frac{1}{2}) \quad (22)$$

where  $a_{m,\mu,p}^+(\mathbf{k})$  and  $a_{m,\mu,p}(\mathbf{k})$  are the creation and annihilation operators, respectively, satisfying bosonic-type commutation relations.

#### 4. Electron–phonon interaction

The Hamiltonian which describes the electron–optical phonon interaction has the form:

$$H_{e-ph} = -e\Phi(\mathbf{x}^e) \quad (23)$$

where  $(-e)$  is the electron charge and  $\Phi(\mathbf{x}^e)$  is the scalar potential (1) generated by the polarization charges only.

Developing the scalar potential in terms of eigenfunctions presented in table 1, the Hamiltonian of interest has the expression:

$$H_{e-ph} = \sum_{\mathbf{k}, m, \mu, p} \exp(i\mathbf{k} \cdot \mathbf{x}_{\perp}^e) \Gamma_{m,\mu,p}(k, l, x_3^e) [a_{m,\mu,p}(\mathbf{k}) + a_{m,\mu,p}^+(-\mathbf{k})] \quad (24)$$

where the coupling functions have the forms:

$$\Gamma_{m,\mu,p}(k, l, x_3^e) = - \left( \frac{\hbar e^2}{2A\omega_{m,\mu,p}} \right)^{1/2} C_{m,\mu,p} F_p(k, \omega_{m,\mu,p}, l, x_3^e) \quad (25a)$$

$$\Gamma_{0,\mu,p}(k, l, x_3^e) = - \left( \frac{\hbar e^2}{2A\omega_{0,\mu,p}} \right)^{1/2} C_{0,\mu,p} F_{0,p}(k, \omega_{0,\mu,p}, l, x_3^e) \quad (25b)$$

$A$  being the area of the heterostructure in the  $(x_1, x_2)$  plane.

For the different domains of the heterostructure the expressions of the functions  $F_j$  are presented in table 2.

In contradistinction with the situation encountered in the case of isotropic heterostructures, in the presence of anisotropy, an electron placed in the isotropic region of a heterostructure interacts with the so-called confined modes. Also, an electron situated inside the anisotropic region interacts with the confined modes having the frequency between  $\omega_{TO,\parallel}^{(1)}$  and  $\omega_{TO,\perp}^{(1)}$ ; in the case of a very thick heterostructure, these modes correspond to the quasi-transverse modes of a 3D anisotropic uniaxial crystal. For a 3D uniaxial crystal, a measure of the interaction strength is given by the angular average of the dimensionless Fröhlich coupling constants,  $\langle \alpha_{\mu}(\theta) \rangle_{AV}$ . Though for a slightly anisotropic crystal of würtzite type like CdS the value of the polaronic constant for these quasi-transverse modes is negligibly small (Brancus and Mocuta 1995), for layered-type semiconductors such as  $\alpha$ -HgI<sub>2</sub> the polaronic constant corresponding to the same type of phononic mode has an unexpectedly large value (Brancus and Stan 1998).

The obtained results can be used to discuss the phonon modes and their interaction with a conduction electron in some hypothetical heterostructures made of layered semiconductors which are strongly anisotropic materials. However, due to their practical importance, we shall present here the case of strained heterostructures made of zincblende-type semiconductors. The induced anisotropy is comparable with the natural anisotropy found in a würtzite-type crystal.

#### 5. Bisotropically strained double heterostructures

Let us consider a double heterostructure containing a zincblende-type semiconductor layer grown on the faces (001) or (111) of the same type of material, 2. For these two cases, as a result of a difference between the lattice parameters of the adjacent materials, a uniaxial



anisotropy of the strained layer appears. In order to avoid the effects induced by the relaxation, we shall assume that the thickness of the strained layer does not exceed a critical thickness.

Compatible with the constraints imposed on the heterostructure geometry which leads to the results previously obtained, we shall assume that the thicknesses of both the buffer and the cladding layers of the heterostructure are, practically, infinite.

In the context of the bisotropic strain model (Anastassakis 1990) for the pseudo-morphic layer, uniaxially distorted, the components  $\varepsilon_{\parallel}^{(1)}$  and  $\varepsilon_{\perp}^{(1)}$  of the dielectric tensor are obtained in terms of the phonon deformation potentials (PDPs),  $K_{ij}^{(L)}$  and  $K_{ij}^{(T)}$ , where L and T are indices standing for longitudinal and transverse optical phonons, and also in terms of low- and high-frequency photoelastic coefficients, respectively.

### 5.1. Heterostructure grown on the face (001)

Following Anastassakis (1994), for this particular geometry of the tensile InP/GaAs/InP DHS (Pistol *et al* 1992), for the parameters of the pseudo-morphic layer one obtains the values:  $\varepsilon_{\parallel}^{(1)}(\infty) = 11.5$ ,  $\varepsilon_{\perp}^{(1)}(\infty) = 11.7$ ,  $\omega_{TO,\parallel}^{(1)} = 252 \text{ cm}^{-1}$ ,  $\omega_{TO,\perp}^{(1)} = 255.6 \text{ cm}^{-1}$ ,  $\omega_{LO,\parallel}^{(1)} = 273.3 \text{ cm}^{-1}$ ,  $\omega_{LO,\perp}^{(1)} = 281.1 \text{ cm}^{-1}$ , the lattice constants being  $a_{InP} = 5.869 \text{ \AA}$  and  $a_{GaAs} = 5.654 \text{ \AA}$ .

The above results have been obtained by considering for InP and unstrained GaAs, the following values of the material parameters:  $\varepsilon^{(2)}(\infty) = 9.61$ ,  $\omega_{TO}^{(2)} = 304 \text{ cm}^{-1}$ ,  $\omega_{LO}^{(2)} = 351 \text{ cm}^{-1}$  and  $\varepsilon^{(1)}(\infty) = 10.9$ ,  $\omega_{TO}^{(1)} = 269 \text{ cm}^{-1}$ ,  $\omega_{LO}^{(1)} = 292 \text{ cm}^{-1}$ , respectively.

In figure 2 the dispersion curves of the interface modes—dotted for an unstrained heterostructure and solid curves for a bisotropically strained heterostructure—are presented for the above-mentioned case. The interface modes occurring in the domain of the *reststrahlen* band of InP (the branch index  $\mu = 1$ ) are modified only to a very little extent by the effect of the strains. The opposite situation is found for the modes which occur in the *reststrahlen* band of GaAs, the frequency domain of which is  $(\omega_{TO}^{(1)}, \omega_{LO}^{(1)})$  for unstrained layer and is well marked by the effect of the strains, becoming  $(\omega_{TO,\perp}^{(1)}, \omega_{LO,\parallel}^{(1)})$ . In a rough estimation, one can say that the dispersion curves for both symmetrical and antisymmetrical interface modes of the branch ( $\mu = 2$ ) are shifted to lower frequencies, as a strain-induced effect, with 14 and 20  $\text{cm}^{-1}$ , respectively.

We have plotted in figure 3 the dispersion curves of the confined mode  $m = 1$ ,  $\mu = 1$ ,  $p = +$ ,  $k$  for two thicknesses of GaAs pseudo-morphic layer obtained by Pistol *et al* (1992). As a effect of the built-in strain distribution the degeneracy of the confined LO phonon modes having the frequency  $\omega_{LO}^{(1)}$  is lifted and the frequencies of these confined modes ( $\mu = 1$ ) are distributed into a frequency domain, which in a (hypothetical) limit of a very thick layer becomes  $(\omega_{LO,\parallel}^{(1)}, \omega_{LO,\perp}^{(1)})$ . A similar effect is also observed for the confined modes having  $\mu = 2$  for the branch index.

In figure 4 we present the effect of the strain distribution on the coupling functions describing the electron–interface-phonon mode interaction by plotting as a function of  $kl$  the relative variation  $\Delta\Gamma_{0,\mu,p}/\Gamma_{0,\mu,p}^{is}$  defined as:

$$\Delta\Gamma_{0,\mu,p}/\Gamma_{0,\mu,p}^{is} = \Gamma_{0,\mu,p}^{str.}(k, l, l/2)/\Gamma_{0,\mu,p}^{is.}(k, l, l/2) - 1 \quad (26)$$

where the labels str. and is. represent the case of a strained and an isotropic heterostructure, respectively. Excepting the modes (0, 1, +) for all the other interface modes of a strained heterostructure one observed a well marked effect of the strain distribution on the strength of the electron–phonon interaction.

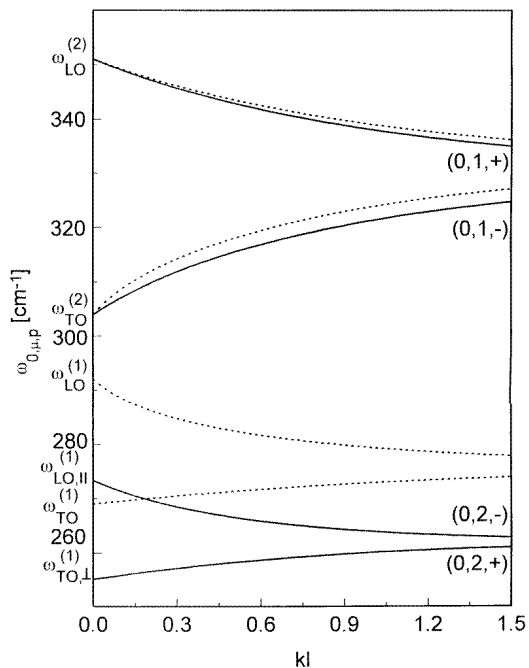


**Figure 2.** Dispersion curves of the interface-phonon modes for an InP/GaAs/InP DHS grown on the face (001). The solid and the dotted curves are for a strained and an unstrained heterostructure, respectively.

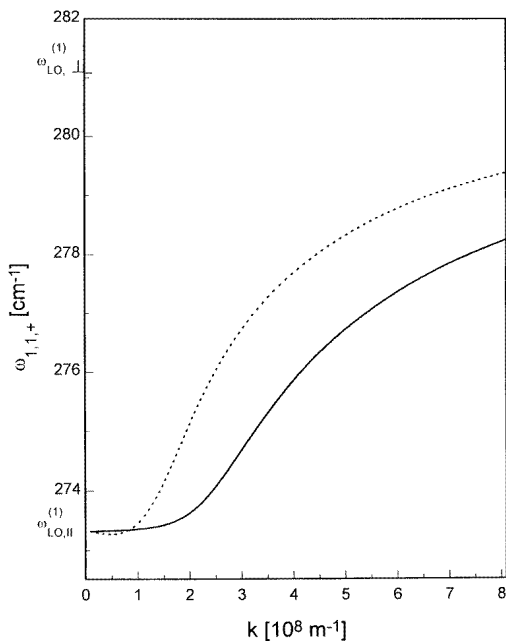


**Figure 3.** Dispersion curves of the confined quasi-longitudinal mode ( $m = 1, \mu = 1, p = +$ ) of a strained InP/GaAs/InP DHS grown on the face (001), for two thicknesses of the pseudo-morphic layer; the dotted and solid curves correspond to  $l = 28 \text{ \AA}$  and  $l = 18 \text{ \AA}$ , respectively.

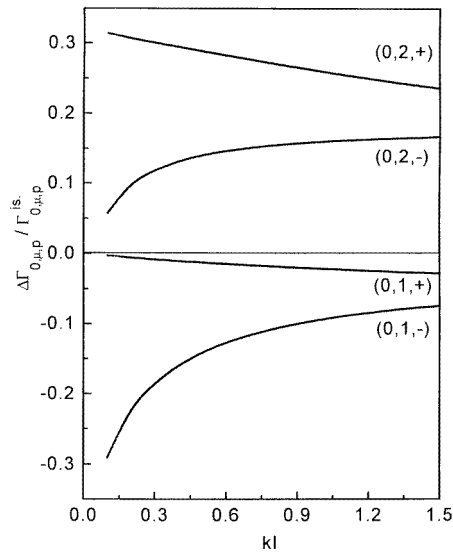


**Figure 4.**  $kl$  dependence of the relative variation  $\Delta\Gamma_{0,\mu,p}/\Gamma_{0,\mu,p}^{is.}(k, l, l/2)$  for all the interface phonon modes of an InP/GaAs/InP DHS grown on the face (001).

For the two DHSs obtained by Pistol *et al* (1992), due to the presence of the strain distribution, the strength of the electron–phonon interaction of the confined modes is modified only to a small extent (as large as 5% for  $l = 18 \text{ \AA}$  and 3.5% for  $l = 28 \text{ \AA}$ ).

### 5.2. Heterostructure grown on the face (111)

To exemplify this particular geometry we shall consider the case of a compressive heterostructure obtained by growing a strained InP layer on the face (111) of a GaAs substrate.

Analogue to the case previously discussed, by particularizing the results of Anastassakis (1994), for the material parameters describing the anisotropic properties of the pseudomorphic InP layer one obtains the values:  $\varepsilon_{\parallel}^{(1)}(\infty) = 9.72$ ,  $\varepsilon_{\perp}^{(1)}(\infty) = 8.9$ ,  $\omega_{TO,\parallel}^{(1)} = 320.3 \text{ cm}^{-1}$ ,  $\omega_{TO,\perp}^{(1)} = 328.7 \text{ cm}^{-1}$ ,  $\omega_{LO,\parallel}^{(1)} = 369 \text{ cm}^{-1}$ ,  $\omega_{LO,\perp}^{(1)} = 372.9 \text{ cm}^{-1}$ .

Using the values of these parameters and based on the relations (14)–(16), the dispersion curves, for the interface phonon modes of this DHS are obtained and presented in figure 5 (the dotted and solid curves are for unstrained and strained heterostructures, respectively). Once again, the effect of the strain distribution on the dispersion curves of the interface-phonon modes affects, mainly, the behaviour of the modes occurring in the *reststrahlen* band of the layer. As compared to the case of a tensile DHS presented in figure 2, for the above-considered compressive heterostructure, the frequencies of the interface modes are shifted towards the domain of higher frequencies with contributions estimated as  $25 \text{ cm}^{-1}$  and  $18 \text{ cm}^{-1}$  for the modes  $(0, 2, +, k)$  and  $(0, 2, -, k)$ , respectively.

In figure 6, for  $kl = 0.2$ , the spatial dependences of the coupling functions of the interaction between a conduction electron and the interface-phonon modes are plotted. The strain distribution affects, mainly, the strength of the electron–phonon interaction for the symmetrical interface modes.

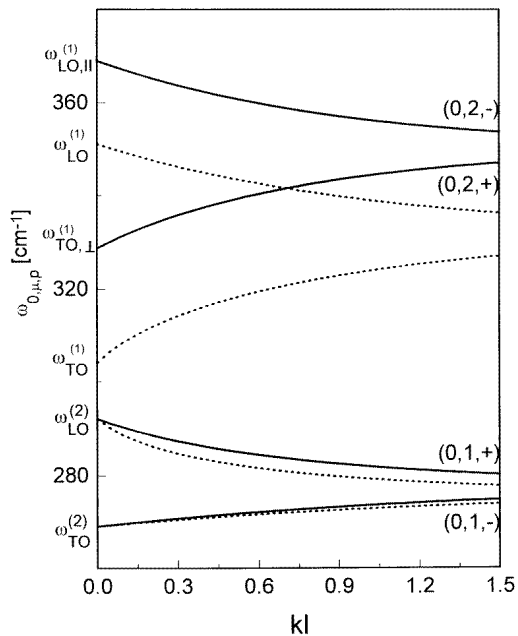


**Figure 5.** Dispersion curves of the interface modes of a GaAs/InP/GaAs DHS grown on the face (111). The solid and the dotted curves are for a strained and an unstrained heterostructure, respectively.

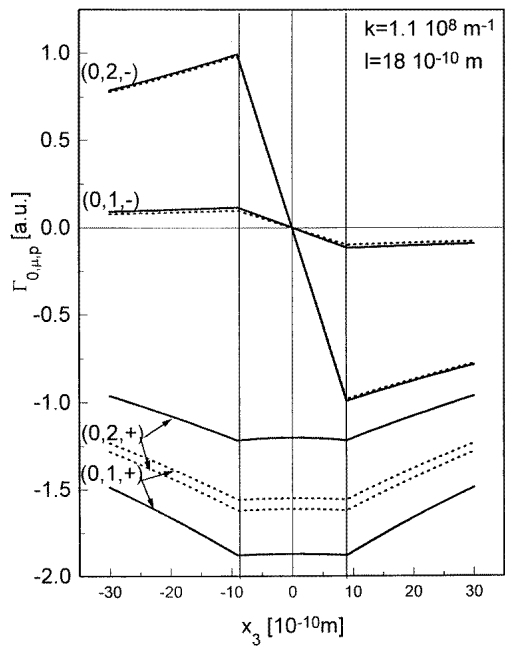


**Figure 6.** Spatial dependence of the coupling functions  $\Gamma_{0,\mu,p}$  of the electron–interface-phonon interactions of a GaAs/InP/GaAs DHS grown on the face (111), with  $l = 18 \text{ \AA}$  and  $kl = 0.2$ . The dotted and the solid curves correspond to an unstrained and a strained heterostructure, respectively.

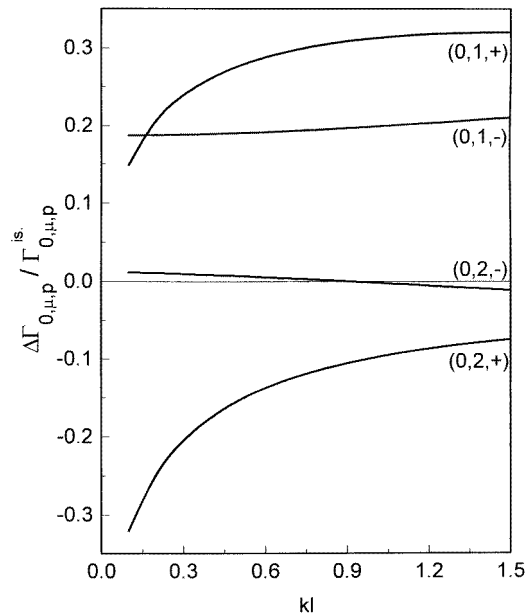


**Figure 7.**  $kl$ -dependence of the relative variation  $\Delta\Gamma_{0,\mu,p}/\Gamma_{0,\mu,p}^{is.}(k, l, l/2)$  for all the interface phonon modes of a GaAs/InP/GaAs DHS grown on the face (111).

Figure 7 presents the  $kl$ -dependence of the relative variation due to the presence of the strain distribution of the coupling functions. Though the effect of the strain distribution on the behaviour of the dispersion law of the modes  $(0, 1, +, k)$  is unimportant, the relative variation of the coupling function for the same modes has a notable value (30%), practically in the whole range of  $k$ . The opposite situation is encountered for the  $(0, 2, -, k)$  modes.

## 6. Conclusions

The dispersion laws and the normal modes of the optical phonons have been obtained in the case of a double semiconductor heterostructure having as interjacent layer a uniaxial polar material with the optical axis directed along the normal to the interface.

We have found also the form of the Hamiltonian describing electron–optical-phonon interactions, thus generalizing, to this anisotropic case, the results presented by Mori and Ando (1989) for isotropic heterostructures. To apply the obtained results to some particular cases we have considered in the context of the bisotropic strain model (Anastassakis 1990) a strained semiconductor double heterostructure, made by zincblende-type semiconductors with pseudo-morphic layer uniaxially distorted by the built-in strain distribution.

The system cumulates both the effect of the anisotropy and that of the confinement. As a result of the anisotropy, the degeneracies of the LO and TO confined modes of an isotropic heterostructure are lifted; thus the obtained quasi-longitudinal and quasi-transverse confined modes have the frequencies distributed into the domains  $(\omega_{LO,\parallel}^{(1)}, \omega_{LO,\perp}^{(1)})$  and  $(\omega_{TO,\parallel}^{(1)}, \omega_{TO,\perp}^{(1)})$ , respectively.

The effect of the built-in strain distribution on the confined modes leads to anisotropic features comparable in magnitude with those found in some slightly anisotropic semiconductors as CdS, InSe. The main effect is obtained on both the dispersion curves of

the interface-phonon modes (see figures 2, 5) and on the coupling functions for the same modes (see figures 4, 6, 7).

The obtained results can be applied in both cases, that of a natural anisotropic heterostructure and that of a strained heterostructure, as well. Referring to this last case we believe that, for very narrow interjacent layers, in discussing the effects determined by the electron-optical-phonon interaction (polaron self-energy, scattering rate), the anisotropic features of the interface-phonon spectra have to be considered in the future.

## References

- Anastassakis E 1990 *J. Appl. Phys.* **68** 4561–8  
—1994 *Acta. Phys. Hung.* **74** 83–105  
Brancus D E N and Mocuta A C 1995 *Can. J. Phys.* **73** 126–30  
Brancus D E N and Stan G 1998 *Phys. Rev. B* **57** 3411–17  
Englman R and Ruppin R 1968 *J. Phys. C (Proc. Phys. Soc.)* **1** 614–29  
Licari J and Evrard R 1977 *Phys. Rev. B* **15** 2254–64  
Los J, Fasolino A and Catellani A 1996 *Phys. Rev. B* **53** 4630–48  
Merten L 1972 *Atomic Structure and Properties of Solids* ed E Burstein (New York: Academic)  
Mori N and Ando T 1989 *Phys. Rev. B* **40** 6175–88  
Pistol M-E, Gerling M, Hessman D and Samuelson L 1992 *Phys. Rev. B* **45** 3628–35  
Ridley B-K, Al-Dossary O, Constantinou N C and Babiker M 1994 *Phys. Rev. B* **50** 11 701–9  
Trallero-Giner C, Garcia-Moliner F, Velasco V R and Cardona M 1992 *Phys. Rev. B* **45** 11 944–8  
Wendler L 1985 *Phys. Status Solidi b* **129** 513–30  
Wendler L and Jäger E 1983 *Phys. Status Solidi b* **120** 235–47